

Polynomial Maximization Method with Fractional Polynomial Basis: A Frequentist Bridge to Bayesian Fractional Polynomials

Serhii Zabolotnii ^{ID} 1,2,3

¹ Cherkasy State Business College, Cherkasy 18028, Ukraine

² State Scientific Research Institute of Armament and Military Equipment Testing and Certification, Cherkasy, Ukraine

³ Uzhhorod National University, Uzhhorod, Ukraine

Address for correspondence: Serhii Zabolotnii, Cherkasy State Business College, 18028 Cherkasy, Ukraine.

Abstract: Fractional polynomials are widely used for dose-response modelling, and recent Bayesian fractional polynomial work has renewed interest in this finite model class. We propose PMM-FP, a frequentist extension of Kunchenko's polynomial maximization method to fractional-polynomial bases, developed in two parallel tracks for positive and full FP power sets under appropriate moment conditions. The main result is the closed-form variance-reduction coefficient $g_2 = 1 - \gamma_3^2 / (2 + \gamma_4)$ relative to OLS-FP for asymmetric non-Gaussian errors, formalised in Lean 4 and validated by Monte Carlo. On GBSG residuals, $\hat{\gamma}_3 = -1.74$, $\hat{\gamma}_4 = 4.91$, $g_2 \approx 0.56$: an expected standard-error gain. PMM-FP is a computationally cheap frequentist bridge to Bayesian FP modelling.

Key words: fractional polynomials; Kunchenko stochastic polynomials; non-Gaussian errors; polynomial maximization method; statistical modelling; variance reduction

1 Introduction

1.1 Dose-response modelling and the role of fractional polynomials

Modelling the dependence of a biological response on dose is a canonical task in biostatistics, toxicology, and pharmacometrics. Standard parametric families (Hill, Michaelis-Menten, Emax) work well when the mechanism is known a priori (Ritz et al., 2015), but in exploratory problems (Crippa et al., 2019) the form $R(\theta, x) = \mathbb{E}[y \mid x]$ is unknown and requires a flexible approximation. Fractional polynomials (FP) (Royston and Altman, 1994) provide such an approximation based on the basis $P = \{-2, -1, -0.5, 0, 0.5, 1, 2, 3\}$ with the convention $x^0 \equiv \ln x$, encompassing classical parametric forms as special cases. The monograph of Royston and Sauerbrei (2008) and a methodological series in *Statistics in Medicine* (Sauerbrei et al., 2007) made FP the de facto standard in clinical statistics (R package `mfp`). Classical FP inherits, however, two limitations of OLS: sensitivity to non-Gaussian errors and the absence of explicit modelling of the error distribution.

1.2 Limitations of OLS-FP and BFP under non-Gaussian errors

In dose-response problems the errors ξ are typically non-Gaussian: log-normal (concentrations), gamma (time-to-event), beta (proportions). For such distributions, OLS-FP is consistent but loses 30–50% efficiency for $|\gamma_3| \geq 1$ compared with an estimator that incorporates γ_3, γ_4 .

Hubin et al. (2026) proposed a Bayesian version of FP (BFP) — power selection via MJMCMC in the space of 2^K subsets, continuing the line of Sabanés Bové and Held (2011). However, BFP retains the Gaussian error model: for asymmetric ξ it inherits the inefficiency of OLS-FP, masked by posterior probabilities. The MJMCMC sampler is computationally expensive compared with a frequentist counterpart. Thus, OLS-FP and BFP share a complementary gap: efficient frequentist estimation under asymmetric errors without OLS assumptions and MCMC machinery. This gap is closed by the method we propose.

1.3 The Polynomial Maximization Method as a framework

The Polynomial Maximization Method (PMM) (Kunchenko, 2002) extends MLE to cases where only a finite sequence of moments is known. For $y_v = R(\theta, X_v) + \xi_v$ with $\mathbb{E}[\xi_v] = 0$, PMM-FP maximises the stochastic functional (Zabolotnii et al., 2025, eq. (2)):

$$L_{SN} = \sum_{v=1}^N \sum_{i=1}^S \phi_i(y_v) \int^a k_{iv}(a) da - \sum_{i=1}^S \sum_{v=1}^N \int^a \Psi_{iv}(a) k_{iv}(a) da, \quad (1.1)$$

where ϕ_i are basis functions, $\Psi_{iv}(a) = \mathbb{E}[\phi_i(y_v)]$, and k_{iv} are chosen variationally. The classical choice $\phi_i(y) = y^i$, $S = 2$ (Zabolotnii et al., 2018, 2019, 2025; Zabolotnii, 2025) with $y_v - a = \xi_v$ yields the second-order variance coefficient in (3.7) (Zabolotnii et al., 2025, eq. (27)). For the integer basis, location equivariance guarantees that the y -basis and ξ -basis yield the *same* g_2 (Kunchenko, 2002, ch. 4).

The Royston-Altman fractional basis introduces two parallel extensions into (1.1): *regressor extension* ($R(\theta, x) = \beta_0 + \sum_k \beta_k x^{p_k}$) and *extension of the score-function basis* ($\{\xi, \xi^2\} \rightarrow \{g_{p_1}(\xi), \dots, g_{p_K}(\xi)\}$). PMM-FP is the joint application of both. We use *Form B* (score-function on the residual, Kunchenko, 2002, ch. 4) with R -independent $\{g_p(\xi)\}$ and scalar g_S . The present work adds the bridge $\text{PMM} \leftrightarrow \text{FP/BFP}$ to Kunchenko's programme of

bridges to neighbouring Western frameworks (SLS (Wang and Leblanc, 2008), GMM (Hansen, 1982), M-estimators (Huber, 1981)), and provides, to our knowledge, the first formal Lean 4 verification of the school’s regression apparatus. The technical question of correctly defining ξ^p for sign-changing ξ is resolved through the *signed-parity* convention (B2) in §3.1.

1.4 Contributions and outline

We present four principal contributions: (1) **a formal bridge from PMM to FP** (the first one to our knowledge) — transferring Kunchenko’s stochastic polynomial apparatus to the Royston-Altman fractional basis in two equal tracks (D1v2): *track* (a) PMM-FP_{pos} with $\mathcal{P}_a = \{0, 0.5, 1, 2, 3\}$ and $\mathbb{E}[\xi^4] < \infty$; *track* (b) PMM-FP_{full} with $\mathcal{P}_b = \{-2, -1, -0.5, 0, 0.5, 1, 2, 3\}$, $K = 16$, and BD0 ($\mathbb{E}[|\xi|^{-2}] < \infty$); track (b) mirrors the model space of Hubin et al. (2026); (2) **extension to $S \geq 3$** — classical FP is restricted to ≤ 2 terms, whereas Kunchenko yields the monotone sequence $g_2 \geq g_3 \geq \dots \geq g_\infty$ (Cramér-Rao); (3) **a Lean 4 formalisation** (we are not aware of prior Lean 4 work on PMM-style estimators) — all theorems T_1^a – T_4^a and T_1^b – T_4^b in Lean 4 + Mathlib v4.26.0 (Lean/PMM_FP/; theorem map in the supplement); (4) **a computationally cheap alternative to BFP** — exhaustive enumeration of models with ≤ 4 terms in $\mathcal{P}_a, \mathcal{P}_b$ ($K_a = 30, K_b = 162$) runs in a fraction of a second, a one-to-two order-of-magnitude computational speedup over MJMCMC (§5.3).

Outline. §2 — background, related literature, and positioning; §3 — theoretical PMM-FP score, assumptions and T_1 – T_4 ; §4 — the PMM-FP estimator and numerical implementation; §5 — simulation comparison and the GBSG application; §6 — discussion; §7 — conclusions. Supplementary material covers extended Lean cross-references and proofs.

2 Background, related literature, and positioning

PMM-FP sits at the intersection of three methodological strands: fractional-polynomial model building, Bayesian model averaging over FP bases, and Kunchenko’s moment-based Polynomial Maximization Method. This section reviews those strands once, then positions the proposed estimator relative to neighbouring estimating-equation, robust, and reproducible-modelling literatures.

2.1 Fractional-polynomial model building

Fractional polynomials were introduced by [Royston and Altman \(1994\)](#) as a parsimonious alternative to splines for modelling smooth nonlinear effects of continuous covariates in biostatistics. The standard finite power set is

$$\mathcal{P}_{\text{full}} = \{-2, -1, -0.5, 0, 0.5, 1, 2, 3\}, \quad (2.1)$$

with $x^0 \equiv \log x$. For $x > 0$, an FP model of degree m is

$$\text{FP}_m(x; \beta, p) = \beta_0 + \sum_{i=1}^m \beta_i x^{p_i}, \quad p_i \in \mathcal{P}_{\text{full}}, \quad (2.2)$$

with repeated powers represented by $\beta_i x^p + \beta_{i+1} x^p \log x$.

The practical success of FP modelling comes from the small and interpretable transformation set, the inclusion of common logarithmic, inverse and quadratic shapes, and the controlled extra curvature available through repeated powers. The multivariable FP programme ([Royston and Sauerbrei, 2008](#); [Sauerbrei et al., 2007](#)) turned this into an applied workflow for variable and functional-form selection, implemented in the R package `mfp`. Canonical FP restricts attention to $m \leq 2$ for parsimony and interpretability, and commonly uses closed testing over $|\mathcal{P}_{\text{full}}|^2 = 64$ second-degree candidates.

The limitation relevant here is not the FP transformation family itself, but the inferential engine usually attached to it. In the standard FP pipeline the transformation space is rich, whereas the error model remains close to ordinary least squares or a generalized linear model. If residuals are strongly skewed or heavy-tailed, the selected FP basis may remain substantively appropriate while the coefficient estimator and its standard errors are inefficient. PMM-FP keeps the finite FP model space but replaces the OLS score by a moment-based score that uses residual skewness and kurtosis directly.

2.2 Bayesian fractional polynomials and the Hubin et al. anchor

Bayesian fractional polynomials add a probability model over the candidate transformations. The formulation of [Sabanés Bové and Held \(2011\)](#) introduced posterior inference over FP structures through priors on a power-inclusion vector and shrinkage priors on regression coefficients. The recent BFP framework of [Hubin et al. \(2026\)](#) scales this idea with mode-jumping MCMC over the full FP basis and applies it to optimal dosage estimation in fish nutrition. In their notation,

$$h(\mathbb{E}[y_i]) = \eta_i = \beta_0 + \sum_{k=1}^K \gamma_k \beta_k f_k(x_i), \quad i = 1, \dots, n, \quad (2.3)$$

where $h(\cdot)$ is a link function, $f_k(\cdot)$ are FP transformations, and $\gamma_k \in \{0, 1\}$ are inclusion indicators. Doubling the powers in (2.1) by x^p and $x^p \log x$ gives $K = 16$ and a model space of size $2^{16} = 65\,536$. The prior structure combines Bernoulli inclusion probabilities with Zellner's g-prior for active coefficients, and posterior model averaging yields inference for the response curve and the optimal dose.

BFP addresses model uncertainty; PMM-FP addresses a different part of the same modelling problem. BFP asks how posterior probability should be distributed over a finite transformation space. PMM-FP asks how to estimate the coefficients of an FP model effi-

ciently when residuals are non-Gaussian and only a finite set of moments is used. The two approaches are therefore complementary. BFP is attractive when the posterior distribution over models or optimal doses is the inferential object; PMM-FP is attractive when fast frequentist estimation and standard-error control under asymmetric errors are central.

The fish-nutrition application of [Hubin et al. \(2026\)](#) is used here as a notational and methodological anchor, not as a replicated dataset. Without the original fish data, the empirical evidence in the present paper is based on reproducible simulations and the public GBSG dataset, while the Hubin et al. paper defines the Bayesian benchmark class.

2.3 PMM as a moment-based estimating framework

Kunchenko's Polynomial Maximization Method ([Kunchenko, 2002](#)) belongs to the broader family of estimators that replace a fully specified likelihood by a finite set of moment conditions. In its classical form, the central object is a stochastic polynomial of order S ,

$$\eta_S(\xi) = h_0 + \sum_{i=1}^S h_i \xi^i, \quad S \in \mathbb{N}, \quad (2.4)$$

with basis $\{\xi, \xi^2, \dots, \xi^S\}$. The coefficients are chosen variationally through centred correlants

$$F_{ij} = \mathbb{E}[\xi^{i+j}] - \mathbb{E}[\xi^i]\mathbb{E}[\xi^j], \quad i, j = 1, \dots, S, \quad (2.5)$$

which leads to the linear system

$$\mathbf{F}\mathbf{h}^* = \mathbf{b}, \quad (2.6)$$

where \mathbf{b} contains the moment-parameter intersections. Substituting the optimal coefficients gives a variance-reduction coefficient

$$g_S = \frac{\text{Var}[\hat{\theta}_{\text{PMM},S}]}{\text{Var}[\hat{\theta}_{\text{OLS}}]}, \quad 0 < g_S \leq 1. \quad (2.7)$$

For $S = 2$ and standardized errors, this gives the PMM2 coefficient in (3.7); hence $g_2 = 1$ in the symmetric Gaussian case and $g_2 < 1$ when skewness contributes additional information.

Previous PMM applications covered asymmetric linear regression (Zabolotnii et al., 2018), symmetric non-Gaussian regression (Zabolotnii et al., 2019), nonlinear regression (Zabolotnii et al., 2025), and time-series models with non-Gaussian innovations (Zabolotnii, 2025).

The current paper extends that pattern from integer stochastic polynomials to fractional polynomial regression. This is not merely a change of notation: fractional powers raise domain and moment-existence questions that do not arise in the integer basis. Positive powers require ordinary finite moments, whereas negative powers require control near zero. This is why PMM-FP has two parallel tracks: a stable positive-power track and a full FP track with bounded-density and inverse-moment assumptions. The broader PATP extension of Kunchenko's apparatus is discussed in Zabolotnii (2026); PMM-FP is the discrete FP-regression specialisation needed for statistical modelling.

2.4 Relation to GMM, Godambe information and quasi-likelihood

From a Western statistical perspective, PMM-FP is closest to estimating-equation and generalized method of moments methodology. In GMM (Hansen, 1982), parameters are estimated by solving sample moment equations and choosing a weighting matrix. PMM-FP can be written in this form, with score functions generated by the fractional residual basis. In just-identified cases the PMM and GMM solutions coincide numerically; in overidentified settings GMM-style diagnostics provide natural checks for misspecification.

The Godambe-information viewpoint (Godambe, 1960) gives a second interpretation. A chosen estimating function has a sandwich information matrix, and optimality is relative to the class of scores one allows. PMM-FP is Godambe-optimal within the Kunchenko score

class generated by the selected basis; it is not claimed to be globally semiparametrically efficient in the sense of [Bickel et al. \(1993\)](#) or [van der Vaart \(1998\)](#). Fully efficient semiparametric procedures can use richer information about the unknown error density, but at the price of estimating that density. PMM-FP deliberately trades this generality for a closed four-moment correction.

Quasi-likelihood ([Wedderburn, 1974](#)) is another neighbouring framework because it uses mean-variance structure without requiring a full likelihood. PMM-FP is stricter in one sense and richer in another: it assumes explicit residual moment conditions beyond the variance, but it can use skewness and kurtosis information that quasi-likelihood does not exploit. Formula (3.7) is the visible consequence of using this higher-order information.

2.5 Robust estimation and the limits of the claim

Robust M-estimation ([Huber, 1981](#)) is a natural comparator because it also modifies the OLS score. The motivation is different: Huber-type scores protect against outliers and distributional contamination, whereas PMM-FP targets efficiency under a moment model with measurable skewness and kurtosis. Robust estimators can dominate when outliers are the main threat; PMM-FP is preferable when the non-Gaussian shape is systematic rather than accidental.

This distinction constrains the claims of the paper. PMM-FP is not a universal robust method, not a replacement for BFP, and not a claim of prediction dominance on every dataset. Its narrower claim is that for FP models with asymmetric non-Gaussian residuals and finite required moments, PMM-FP supplies a computable frequentist score with an explicit variance-reduction coefficient. The empirical sections are therefore interpreted through standard-error behaviour and matched- basis variance ratios, not through an unconditional

assertion of lower prediction error.

2.6 Model selection and reproducible statistical modelling

FP modelling is inseparable from model selection. Classical FP uses closed testing and information criteria; Bayesian FP uses posterior model probabilities; PMM-FP uses BIC over the same finite power blocks so that score comparison remains transparent. BIC consistency (Schwarz, 1978) provides the asymptotic reference point, while AIC (Akaike, 1973) remains useful in exploratory sensitivity checks. The main selection rule is intentionally simple because the methodological contribution is the estimating score, not a new search algorithm over FP transformations.

Finally, the paper is positioned as a reproducible statistical- modelling contribution. The Lean layer records definitions and algebraic theorem structure; R scripts regenerate simulation and GBSG outputs; the supplement records software versions and data availability. This does not replace statistical evidence, but it reduces ambiguity about what is proved, what is simulated, and what is only a future extension. For a methodology journal, that separation is part of the contribution.

3 Theory

3.1 Theoretical object

The theory is stated for a fixed selected FP block and then extended to finite BIC selection. This separation is important: the PMM argument is about the estimating score for a given fractional-polynomial regression surface, whereas BIC only chooses which finite block is

used. We work with the regression model

$$y_i = R(x_i; \theta) + \xi_i, \quad \mathbb{E}[\xi_i] = 0, \quad (3.1)$$

and fractional-polynomial surfaces built from

$$f_p(x) = \begin{cases} x^p, & p \neq 0, \\ \log x, & p = 0, \end{cases} \quad \mathcal{P}_a = \{0, 0.5, 1, 2, 3\}, \quad \mathcal{P}_b = \{-2, -1, -0.5, 0, 0.5, 1, 2, 3\}.$$

For residual powers we use the signed-parity convention

$$g_p^+(\xi) = |\xi|^p, \quad g_p^-(\xi) = \text{sign}(\xi)|\xi|^p.$$

Let

$$\mathbf{D}_i(\theta) = \nabla_{\theta} R(x_i; \theta), \quad \xi_i(\theta) = y_i - R(x_i; \theta),$$

and let $B = (q_1, \dots, q_K)$ be a signed-parity residual score basis, where each $q_j(\xi) = g_{p_j}^{\tau_j}(\xi)$ with $\tau_j \in \{+, -\}$. The residual score bases used by the two tracks are encoded as the Lean lists `basisA` and `basisB`; the odd logarithmic term g_0^- is excluded because it is not a meaningful residual score.

For a residual distribution μ define

$$\mathbf{F}_B = \text{Cov}_{\mu}\{B(\xi)\}, \quad (3.2)$$

$$\mathbf{b}_B = -\mathbb{E}_{\mu}\{\partial_{\xi} B(\xi)\}, \quad (3.3)$$

$$\psi_B(\xi) = \mathbf{b}_B^{\top} \mathbf{F}_B^{-1} \{B(\xi) - \mathbb{E}_{\mu} B(\xi)\}. \quad (3.4)$$

The resulting PMM-FP estimating equation is

$$\Psi_n(\theta) = \frac{1}{n} \sum_{i=1}^n \psi_B\{\xi_i(\theta)\} \mathbf{D}_i(\theta) = 0. \quad (3.5)$$

The scalar variance-reduction invariant is

$$g(B) = \frac{1}{\sigma^2 \mathbf{b}_B^{\top} \mathbf{F}_B^{-1} \mathbf{b}_B}, \quad \sigma^2 = \text{Var}(\xi). \quad (3.6)$$

Equations (3.2)–(3.6) are the mathematical presentation of the Lean definitions for correlants, derivative vectors and the scalar reduction factor. They also show why the full track needs inverse-moment diagnostics: negative powers enter both \mathbf{F}_B and \mathbf{b}_B .

3.2 Regularity assumptions

The following regularity conditions are assumed throughout.

(A1) Sampling and design.

Observations are independent, the design is fixed or independent of the errors, and $n^{-1} \sum_i \mathbf{D}_i(\theta_0) \mathbf{D}_i(\theta_0)^\top \rightarrow \mathbf{G}$ with \mathbf{G} positive definite.

(A2) Local FP identifiability.

The selected FP block has a unique parameter vector θ_0 in a compact neighbourhood, and the population estimating equation has a unique zero at θ_0 .

(A3) Differentiability.

$R(x; \theta)$ is twice continuously differentiable in a neighbourhood of θ_0 , and the derivatives are dominated by an integrable envelope.

(A4a) Positive-track moments.

For PMM-FP_{pos}, the residual has finite fourth moment and the signed-parity score functions in basisA are square-integrable.

(A4b) Full-track moments.

For PMM-FP_{full}, BD0 holds in the operational sense: the negative-power score functions in basisB and their squares are integrable. This includes the inverse-moment checks used in the empirical diagnostics.

(A5) Score nonsingularity.

\mathbf{F}_B is nonsingular and $\mathbf{b}_B^\top \mathbf{F}_B^{-1} \mathbf{b}_B > 0$.

(A6) Standard M-estimation regularity.

The uniform law of large numbers and the central limit theorem apply to the score in (3.5). We use the usual M-estimator reduction of van der Vaart (1998, Theorems 5.7 and 5.21).

Track (a) uses (A1)–(A3), (A4a), (A5)–(A6). Track (b) replaces (A4a) by (A4b). The assumptions are intentionally stronger than a minimal theorem would require; their role is to make the submission transparent and to keep the positive and full tracks parallel.

3.3 Consistency and asymptotic distribution

Theorem 3.1 (Consistency, tracks (a) and (b)). *For a fixed correctly specified FP block, under the corresponding assumptions above, the PMM-FP estimator solving (3.5) satisfies*

$$\hat{\theta}_n \xrightarrow{\mathbb{P}} \theta_0.$$

Proof sketch. The estimator is an M-estimator. Assumptions (A1)–(A5) give a unique population zero and local nonsingularity. Assumption (A6) gives uniform convergence of Ψ_n to its population counterpart, so the M-estimator consistency theorem of van der Vaart (1998, Theorem 5.7) applies. In Lean this reduction is recorded in Consistency.lean: identifiability of the signed-parity score basis is verified directly, while the uniform-LLN step is supplied as an explicit assumption in the Lean formalization. \square

Theorem 3.2 (Asymptotic normality, tracks (a) and (b)). *Under the assumptions of Theorem 3.1, plus differentiability of the Jacobian in a neighbourhood of θ_0 ,*

$$\sqrt{n}(\hat{\theta}_n - \theta_0) \xrightarrow{d} N\{0, \mathbf{A}^{-1} \mathbf{C} (\mathbf{A}^{-1})^\top\},$$

where

$$\mathbf{A} = \mathbb{E}\{\partial_\theta[\psi_B(\xi(\theta))\mathbf{D}(\theta)]_{\theta=\theta_0}\}, \quad \mathbf{C} = \text{Var}\{\psi_B(\xi)\mathbf{D}(\theta_0)\}.$$

In the homoskedastic fixed-design case this reduces to

$$\sqrt{n}(\hat{\theta}_n - \theta_0) \xrightarrow{d} N\{0, \sigma^2 g(B)\mathbf{G}^{-1}\}.$$

Proof sketch. Expand $\Psi_n(\hat{\theta}_n)$ around θ_0 :

$$0 = \Psi_n(\theta_0) + \dot{\Psi}_n(\tilde{\theta}_n)(\hat{\theta}_n - \theta_0).$$

The first term obeys a multivariate CLT; the derivative term converges to \mathbf{A} by the LLN and nonsingularity. Slutsky's theorem gives the sandwich covariance. The scalar reduction to $\sigma^2 g(B)\mathbf{G}^{-1}$ follows from the optimal PMM score (3.4). The Lean asymptotic-normality module records the conditional theorem structure and the non-negativity of the limiting scalar covariance. \square

3.4 Variance reduction: the main PMM-FP result

Theorem 3.3 (Classical PMM2 reduction). *For the two-element Kunchenko basis $B_2 = \{g_1^-, g_2^+\} = \{\xi, \xi^2\}$ and standardized residuals,*

$$g(B_2) = 1 - \frac{\gamma_3^2}{2 + \gamma_4} \equiv g_2. \quad (3.7)$$

Consequently $g_2 \leq 1$, with equality if and only if $\gamma_3 = 0$.

Proof sketch. For standardized errors, the centred correlant matrix of (ξ, ξ^2) is

$$\mathbf{F}_2 = \begin{pmatrix} 1 & \gamma_3 \\ \gamma_3 & 2 + \gamma_4 \end{pmatrix},$$

and the derivative vector is $\mathbf{b}_2 = (1, 0)^\top$ up to the sign convention used in (3.3). Substituting \mathbf{F}_2^{-1} into (3.6) yields (3.7). The algebraic identity is verified in Lean's Setup.lean and the inequalities g2_le_one and g2_eq_one_iff_symmetric in VarianceReduction.lean. \square

Theorem 3.4 (PMM-FP variance reduction, tracks (a) and (b)). *Let B be either basisA or basisB, and assume the corresponding moment and nonsingularity conditions. The asymptotic variance of PMM-FP relative to OLS-FP for the same selected FP block is*

$$\frac{\text{avar}(\hat{\theta}_{\text{PMM-FP}})}{\text{avar}(\hat{\theta}_{\text{OLS-FP}})} = g(B).$$

If $B_2 \subseteq B$ and the Schur-complement regularity condition for the enlarged correlant matrix holds, then

$$g(B) \leq g(B_2) = g_2,$$

with g_2 defined in (3.7).

Proof sketch. The first identity is the fixed-block covariance reduction in Theorem 3.2. For the monotonicity statement, write the enlarged correlant matrix in block form,

$$\mathbf{F}_B = \begin{pmatrix} \mathbf{F}_2 & \mathbf{F}_{12} \\ \mathbf{F}_{21} & \mathbf{F}_{22} \end{pmatrix}.$$

The Schur-complement formula for positive definite block matrices (Boyd and Vandenberghe, 2004, Appendix A.5.5) implies

$$\mathbf{b}_B^\top \mathbf{F}_B^{-1} \mathbf{b}_B \geq \mathbf{b}_2^\top \mathbf{F}_2^{-1} \mathbf{b}_2.$$

Since $g(B) = 1/\{\sigma^2 \mathbf{b}_B^\top \mathbf{F}_B^{-1} \mathbf{b}_B\}$, adding admissible score functions cannot increase the variance ratio. The Lean higher-order module keeps this Schur-complement monotonicity as an explicit input hypothesis because Mathlib lacks the needed matrix theorem in this form. \square

Section 5.2 reports the corresponding empirical plug-in value for the GBSG residuals; it is a variance-ratio prediction for matched FP blocks, not a claim that PMM-FP dominates every possible predictive method on every dataset.

3.5 Model selection and higher-order extension

Proposition 3.5 (BIC selection over finite FP blocks). *Suppose the candidate FP blocks are finite, the true block is identifiable, and underfitted blocks are separated from the population optimum. Then BIC over the PMM-FP fitted blocks selects the true block with probability tending to one.*

Proof sketch. This is the standard Schwarz argument (Schwarz, 1978). For underfitted blocks the population criterion gap is of order n ; for overfitted blocks the stochastic improvement is dominated by the dimension penalty $k \log n$. The Lean model-selection module records this as a conditional theorem with the BIC-consistency step supplied as an explicit statistical input. \square

Proposition 3.6 (Higher-order score progression). *For nested admissible PMM score bases $B_2 \subseteq B_3 \subseteq \dots$ satisfying the same moment and Schur-complement conditions,*

$$1 \geq g(B_2) \geq g(B_3) \geq \dots$$

The practical implication is conservative. Higher-order PMM-FP scores can only improve the ideal asymptotic variance ratio under the stated matrix conditions, but they require higher moments and more stable correlant-matrix estimation. The submitted implementation therefore uses the second-order score for the main evidence and reports higher-order extension as theory plus reproducibility hooks, not as an unqualified finite-sample recommendation.

3.6 Formalisation boundary

The Lean 4 source under Lean/PMM_FP/ builds with Mathlib v4.26.0. Its role is precise but deliberately bounded:

- definitions of the two FP power sets, signed-parity residual scores, centred correlants, \mathbf{b}_B and $g(B)$ are formalised;
- the algebraic PMM2 identity and the basic g_2 inequalities are proved directly;
- consistency, asymptotic normality, BIC selection and Schur-complement monotonicity are encoded as conditional theorem bundles linked to standard external statistical theorems.

Thus the manuscript claims machine-checked algebra and a formal record of theorem structure, not a fully machine-proved M-estimator CLT or a complete formalisation of Schur-complement matrix analysis.

4 PMM-FP estimator and numerical implementation

4.1 Two fractional-polynomial tracks

For numerical fitting, PMM-FP implements model (3.1) through the fractional-polynomial predictor

$$R(x; \beta, p) = \beta_0 + \sum_{k=1}^m \beta_k f_{p_k}(x), \quad f_p(x) = \begin{cases} x^p, & p \neq 0, \\ \log x, & p = 0, \end{cases}$$

and replaces the OLS score by Kunchenko moment scores built from the residual basis. We use two tracks throughout the paper:

$$\mathcal{P}_a = \{0, 0.5, 1, 2, 3\}, \quad \mathcal{P}_b = \{-2, -1, -0.5, 0, 0.5, 1, 2, 3\}.$$

Track (a), PMM-FP_{pos}, avoids negative powers and needs only finite fourth moments. Track (b), PMM-FP_{full}, mirrors the $K = 16$ basis of [Hubin et al. \(2026\)](#) and requires bounded density near zero and finite inverse moments. The signed-parity convention from the PATP framework ([Zabolotnii, 2026](#)) is used when fractional powers are applied to sign-changing residuals:

$$g_p^+(\xi) = |\xi|^p, \quad g_p^-(\xi) = \text{sign}(\xi)|\xi|^p.$$

4.2 Estimating score

For a candidate FP block $M = \{p_1, \dots, p_m\}$, let \mathbf{X}_M be the corresponding FP design matrix with columns $1, f_{p_1}(x), \dots, f_{p_m}(x)$. PMM-FP starts from the OLS-FP coefficient vector

$$\hat{\beta}_M^{(0)} = (\mathbf{X}_M^\top \mathbf{X}_M)^{-1} \mathbf{X}_M^\top y,$$

computes residuals $e_i^{(0)} = y_i - \mathbf{X}_{M,i} \hat{\beta}_M^{(0)}$, and estimates the residual cumulants $\hat{\gamma}_3, \hat{\gamma}_4$. In the second-order Form A score used for the main finite-sample results, the standardized residual $u_i(\beta) = e_i(\beta)/\hat{\sigma}$ is transformed by

$$\psi_2\{u_i(\beta)\} = u_i(\beta) - \frac{\hat{\gamma}_3}{2 + \hat{\gamma}_4} \{u_i(\beta)^2 - 1\}.$$

The PMM-FP coefficient estimate solves the estimating equation

$$\Psi_n(\theta) = \frac{1}{n} \sum_{i=1}^n \psi_2\{u_i(\theta)\} \nabla_\theta R(x_i; \theta) = 0.$$

This score is the two-term Kunchenko projection of the OLS score onto the residual moment basis. It is the computational form behind the closed-form expression in [\(3.7\)](#).

4.3 Numerical solution for coefficient estimates

The coefficient estimate for each candidate block is obtained via a damped Newton/Fisher-scoring iteration. With residual vector $e^{(t)} = y - \mathbf{X}_M \boldsymbol{\beta}^{(t)}$ and score vector $\mathbf{s}_i^{(t)} = \psi_2\{e_i^{(t)}/\hat{\sigma}\}$, define

$$\mathbf{U}_t = \mathbf{X}_M^\top \mathbf{s}^{(t)}, \quad \mathbf{H}_t = \mathbf{X}_M^\top \mathbf{W}_t \mathbf{X}_M,$$

where \mathbf{W}_t is the diagonal derivative weight matrix induced by $\partial\psi_2(u)/\partial u = 1 - 2\hat{a}u$ and $\hat{a} = \hat{\gamma}_3/(2 + \hat{\gamma}_4)$. The update is

$$\boldsymbol{\beta}^{(t+1)} = \boldsymbol{\beta}^{(t)} + \lambda_t \mathbf{H}_t^{-1} \mathbf{U}_t, \quad 0 < \lambda_t \leq 1,$$

where λ_t is chosen by step halving if the PMM objective or the residual scale deteriorates. The iteration stops when both $\|\mathbf{U}_t\|_\infty$ and $\|\boldsymbol{\beta}^{(t+1)} - \boldsymbol{\beta}^{(t)}\|_\infty$ fall below the numerical tolerance, or when a fixed iteration cap is reached. If \mathbf{H}_t is nearly singular, the implementation switches to a ridge linear solve $(\mathbf{H}_t + \tau I)^{-1} \mathbf{U}_t$ and records the event as a conditioning diagnostic.

The resulting algorithm is summarised in Algorithm 1.

4.4 Model enumeration and stability checks

The submitted implementation restricts the main search to FP blocks with at most four terms. This keeps the model space finite and makes exhaustive enumeration feasible for the sample sizes considered here. For a fitted candidate M with k_M coefficients, the selection score is

$$\text{BIC}(M) = n \log\{\text{RSS}(M)/n\} + k_M \log n,$$

computed from the residual sum of squares of the fitted PMM-FP block. The same candidate set is used for OLS-FP comparisons, so the reported differences are driven by the estimating score rather than by a wider model search.

Algorithm 1 PMM-FP: fit and select over candidate FP blocks

Require: data (y, \mathbf{X}) , power-block set $\mathcal{B} \subseteq \binom{[p]}{m}$, tolerance ε , bootstrap replications B
Ensure: best-block estimate $\hat{\beta}_{\text{PMM}}$, diagnostic \hat{g}_2

- 1: **for** each candidate power block $\mathbf{p} \in \mathcal{B}$ **do**
 - 2: Build FP design matrix $\mathbf{X}_{\mathbf{p}}$
 - 3: $\hat{\beta}^{(0)} \leftarrow (\mathbf{X}_{\mathbf{p}}^{\top} \mathbf{X}_{\mathbf{p}})^{-1} \mathbf{X}_{\mathbf{p}}^{\top} y$ ▷ OLS-FP initialisation
 - 4: Estimate $\hat{\sigma}^2, \hat{\gamma}_3, \hat{\gamma}_4$ from residuals $\hat{\xi} \leftarrow y - \mathbf{X}_{\mathbf{p}} \hat{\beta}^{(0)}$
 - 5: $t \leftarrow 0$
 - 6: **repeat**
 - 7: Compute PMM2 score \mathbf{U}_t and approximate Hessian \mathbf{H}_t
 - 8: $\hat{\beta}^{(t+1)} \leftarrow \hat{\beta}^{(t)} + \lambda(\mathbf{H}_t + \tau I)^{-1} \mathbf{U}_t$ ▷ damped Newton/scoring step
 - 9: $t \leftarrow t + 1$
 - 10: **until** $\|\mathbf{U}_t\|_{\infty} < \varepsilon$ **and** $\|\hat{\beta}^{(t)} - \hat{\beta}^{(t-1)}\|_{\infty} < \varepsilon$, or iteration cap reached
 - 11: $\hat{\beta}_{\mathbf{p}} \leftarrow \hat{\beta}^{(t)}$
 - 12: Compute bootstrap SEs over B resamples; $\hat{g}_2 \leftarrow 1 - \hat{\gamma}_3^2 / (2 + \hat{\gamma}_4)$
 - 13: Record $\text{BIC}(\mathbf{p})$
 - 14: **end for**
 - 15: **return** $\hat{\beta}_{\mathbf{p}^*}$ where $\mathbf{p}^* \leftarrow \arg \min_{\mathbf{p} \in \mathcal{B}} \text{BIC}(\mathbf{p})$
-

Form B uses the full signed-parity residual basis and therefore requires the empirical correlant matrix \mathbf{F}_B and derivative vector \mathbf{b}_B . Its native numerical estimate is

$$\hat{g}(B) = \{\hat{\sigma}^2 \hat{\mathbf{b}}_B^\top \hat{\mathbf{F}}_B^{-1} \hat{\mathbf{b}}_B\}^{-1}.$$

For negative powers this matrix can be ill-conditioned at sample sizes typical in practice. We therefore report singular values, condition numbers and Tikhonov-stabilised values $\hat{\mathbf{F}}_{B,\tau} = \hat{\mathbf{F}}_B + \tau I$. If the full-basis condition number is large or the stabilised $\hat{g}(B)$ is dominated by τ , the paper uses PMM-FP_{pos} for coefficient inference and reports the full-basis calculation only as a diagnostic. This is exactly what happens in the GBSG application.

5 Empirical evidence

5.1 Monte Carlo design and visual check

The simulation study compares OLS-FP, PMM-FP, Huber-FP, GMM-FP and a BFP benchmark on matched fractional-polynomial bases. The DGPs cover Gaussian, beta, gamma, exponential and log-normal residual regimes, with sample sizes from small biostatistical studies to moderate epidemiological subsamples. The main estimand is the slope coefficient, and the central diagnostic is

$$\hat{g}_2 = \widehat{\text{Var}}(\hat{\beta}_{\text{PMM}}) / \widehat{\text{Var}}(\hat{\beta}_{\text{OLS}}),$$

reported together with MSE, coverage and runtime. The scripts and stored summaries are regenerated through `supplement/run_all.R`. The design is intentionally matched-basis: the comparison isolates the estimating score rather than giving any method an advantage through a different transformation search.

Table 1 and Figure 1 show the same pattern from two angles. Figure 1 visualises the

Table 1: Matched-basis Monte Carlo summary at large n . Values are empirical \hat{g}_2 for PMM-FP and theoretical g_2 .

DGP	n	PMM-FP \hat{g}_2	theoretical g_2
Gaussian	1000	1.004	1.000
Beta(2,5)	1000	0.792	0.811
Gamma(3)	1000	0.677	0.666
Exponential	1000	0.492	0.500
Log-normal	1000	0.436	0.661

large-sample calibration point, while the supplement records the full sample-size grid. The first four regimes approach the theoretical coefficient as n grows. Gaussian errors stay close to $g_2 = 1$, so PMM-FP does not invent a gain when the OLS score is already appropriate. Beta, gamma and exponential errors move toward the predicted variance reductions. The log-normal regime is retained as a stress case: extreme kurtosis makes plug-in cumulant estimates unstable, so bootstrap diagnostics are more reliable than the closed-form approximation.

5.2 GBSG application

The real-data illustration uses the German Breast Cancer Study Group dataset from the R package `mfp`. The complete-case analysis has $n = 686$. We model $y = \log(\text{rfst})$ against tumour size, hormonal therapy and age, and use the tumour-size FP term as the main real-data coefficient because it is the clinically interpretable continuous predictor. Residuals from the baseline model are strongly non-Gaussian: $\hat{\gamma}_3 = -1.7436$, $\hat{\gamma}_4 = 4.9143$, and the Shapiro-Wilk test rejects normality ($W = 0.870$, $p < 10^{-22}$). Substituting these values into (3.7) gives $\hat{g}_2 \approx 0.5603$. The interpretation is an expected standard-error gain, not a

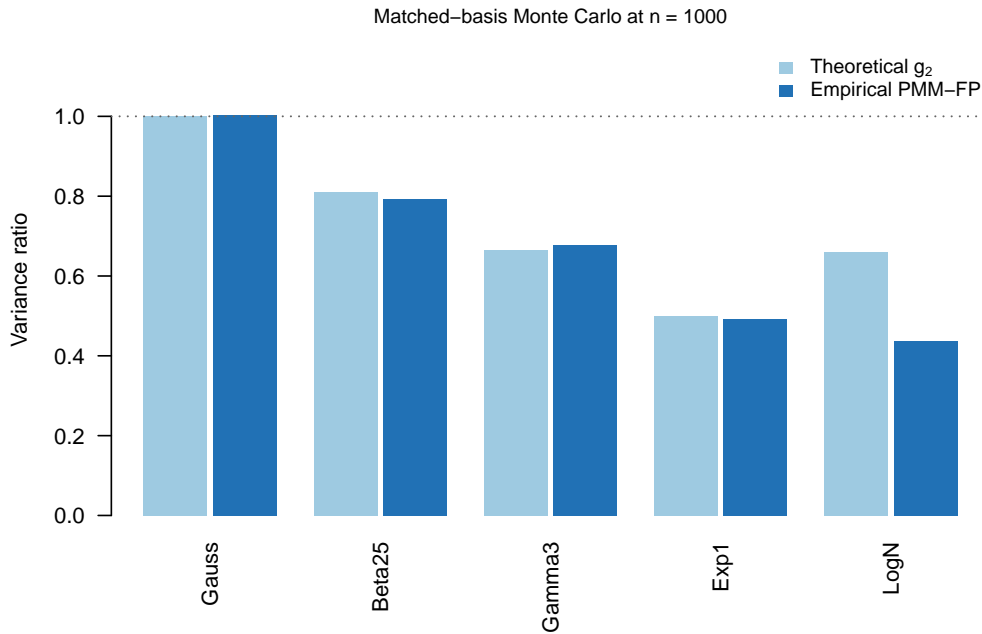


Figure 1: Large-sample Monte Carlo calibration at $n = 1000$. For each DGP, the light bar shows the theoretical variance-reduction coefficient $g_2 = 1 - \gamma_3^2 / (2 + \gamma_4)$ and the dark bar shows the empirical PMM-FP variance ratio for the slope coefficient. The dotted reference line at 1 marks parity with OLS-FP.

claim that PMM-FP universally improves prediction.

The application has three practical messages. First, the fitted curves in Figure 2A remain visually close, so the main question is coefficient stability, not a dramatic change in the fitted mean surface. Second, the bootstrap intervals in Table 2 and Figure 2B show the PMM-FP_{pos} standard-error reduction for the tumour-size coefficient. The density strips above each interval line in Figure 2B display the full bootstrap distribution of $\hat{\beta}_{\text{tum}}$ across 2000 replicates. The OLS-FP strip is wide with heavy tails: most replicates cluster near the median, but occasional extreme draws inflate the standard error to $\text{SE} = 0.118$ while keeping the 95% percentile interval narrow (width 0.121, versus $2 \times 1.96 \times 0.118 = 0.462$ for a Gaussian of the same variance). The PMM-FP strip is markedly more symmetric and

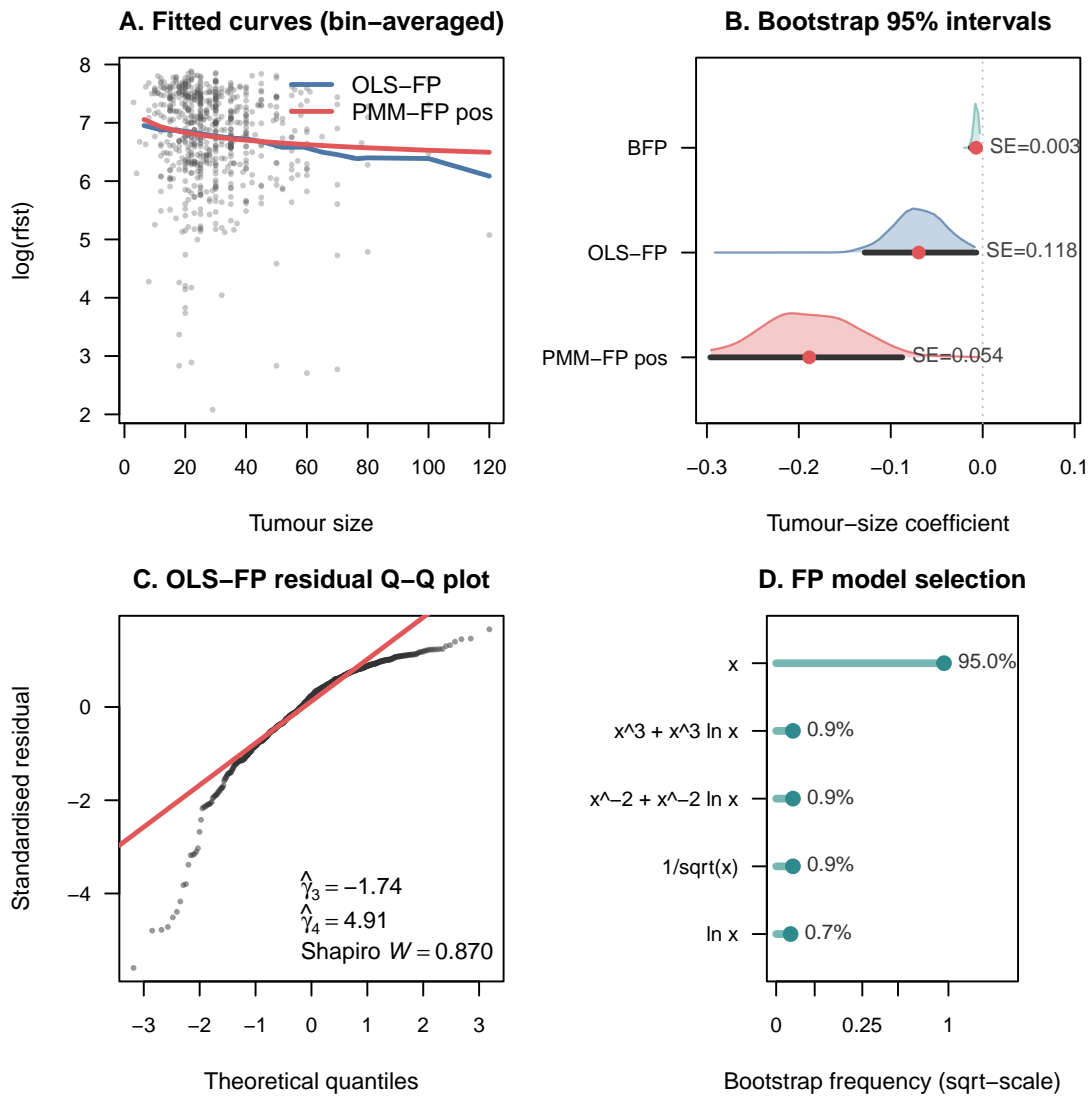


Figure 2: GBSG real-data evidence. **Panel A:** bin-averaged partial dependence of fitted curves on tumour size for OLS-FP and PMM-FP_{pos} (PMM-FP_{full} omitted because its small-sample conditioning is documented as unstable in §4.4). **Panel B:** bootstrap 95% percentile intervals for the tumour-size coefficient, with bootstrap SE annotated. **Panel C:** normal Q-Q plot of standardised OLS-FP residuals (heavy left tail, $\hat{\gamma}_3 = -1.74$, $\hat{\gamma}_4 = 4.91$, Shapiro–Wilk $W = 0.870$) motivating the PMM-FP correction. **Panel D:** top bootstrap FP model-selection frequencies with decoded power-block labels.

Table 2: GBSG ($n = 686$): estimate of the tumsize coefficient and goodness-of-fit measures. Bootstrap $B = 2000$, percentile 95 % CI. Residual deviance is $\sum (y_i - \hat{y}_i)^2$ on the full sample.

Method	$\hat{\beta}_{\text{tum}}$	SE_{boot}	95 % CI	Residual dev.	R^2
OLS-FP	-0.0696	0.1176	[-0.1284, -0.0069]	470.17	0.0265
PMM-FP _{pos} (a)	-0.1887	0.0535	[-0.2963, -0.0875]	476.47	0.0134
BFP	-0.0072	0.0026	[-0.0129, -0.0031]	475.78	0.0149

compact: its percentile interval width (0.208) agrees closely with the normal approximation ($2 \times 1.96 \times 0.054 = 0.212$), confirming that correcting for residual skewness stabilises the bootstrap distribution. The empirical SE ratio, $(0.054/0.118)^2 \approx 0.21$, is smaller than the plug-in coefficient $\hat{g}_2 \approx 0.56$ because PMM-FP also shifts the point estimate ($\hat{\beta}_{\text{OLS}} = -0.070$ versus $\hat{\beta}_{\text{PMM}} = -0.189$): reweighting the skewed-residual contribution moves the estimating-equation root, and the plug-in ratio applies to the fixed-block asymptotic covariance rather than to the bootstrap variance of the realised estimator. Both views agree qualitatively that PMM-FP reduces sampling variability for this coefficient. Third, the model-selection panel shows that classical FP selects the linear tumour-size term in 94.95% of bootstrap replications. PMM-FP is therefore best read as an efficiency correction for a stable predictor structure rather than a device that changes the biological functional form.

We also ran Form B negative-power diagnostics. The positive signed- parity score basis already has a large condition number (3.8×10^6), and the full negative-power basis is worse (2.3×10^{10} before Tikhonov regularisation). The resulting Form B variance ratios are numerically dominated by conditioning. This supports the conservative rule used in the paper: for real data of this size, PMM-FP_{pos} is the default unless BD0 and inverse moments are empirically stable.

5.3 Fish-nutrition anchor

[Hubin et al. \(2026\)](#) provide the Bayesian fractional-polynomial anchor and the notation for the full $K = 16$ basis. Their fish-nutrition data are not redistributed in this repository and are not analysed here. Consequently, the present paper does not claim a direct replication of the vitamin A experiment; it positions PMM-FP as a frequentist companion and comparator to BFP.

6 Discussion

6.1 Interpretation of the contribution

PMM-FP is an estimating-score contribution, not a new fractional-polynomial search algorithm. Classical FP, BFP and the present method can use the same candidate power blocks; PMM-FP changes the post-selection score by replacing the Gaussian least-squares score with a Kunchenko moment score controlled by residual cumulants. Thus the reported gains come from the estimating equation on a matched FP basis, not from a richer model class.

The most interpretable object produced by this construction is the variance-ratio coefficient. In the second-order case, (3.7) is not merely a diagnostic fitted after the fact; it is the scalar coefficient in the fixed-block asymptotic covariance. It answers a practical dose-response question: when residual asymmetry is systematic rather than a small contamination artefact, how much coefficient-variance reduction should one expect from replacing the OLS score? The answer is distributional, transparent and reproducible from the residual cumulants.

6.2 Practical use

The applied recommendation is conservative. Track (a), $\text{PMM-FP}_{\text{pos}}$, should be the default reporting track unless the full negative-power residual basis is well conditioned. It avoids inverse moments and, in the GBSG application, gives the relevant standard-error reduction while preserving the selected functional form. Track (b), $\text{PMM-FP}_{\text{full}}$, remains a main theoretical contribution because it mirrors the full Royston–Altman and Hubin et al. power set, but its applied role is diagnostic: it shows when BDO or inverse-moment instability makes negative powers too fragile.

The empirical section should be read in this light. The simulations validate g_2 in regular asymmetric settings and expose the log-normal case as a cumulant-instability stress test. The GBSG analysis shows the same pattern in real data: residual skewness predicts a material standard-error gain, while the full negative-power matrix is too ill-conditioned to be the preferred finite-sample estimator. The claim is coefficient-efficiency improvement under explicit moment and conditioning requirements, not universal prediction dominance.

6.3 Relation to neighbouring frameworks

The method complements BFP, robust M-estimation and GMM. BFP is preferable for posterior uncertainty over model space; PMM-FP is preferable for fast frequentist estimation and direct efficiency diagnostics under non-Gaussian residuals. Robust M-estimators ([Huber, 1981](#)) target outliers and contamination, whereas PMM-FP targets systematic skewness and kurtosis. The GMM connection ([Hansen, 1982](#)) is useful because PMM-FP is an estimating-equation method with a residual score basis and correlant weighting matrix, while Kunchenko’s construction supplies the closed variance-reduction coefficient and higher-order score progression.

The PATP preprint (Zabolotnii, 2026) provides the broader signed-parity and continuous- α foundation. PMM-FP is the statistical-modelling specialization of that programme: fixed FP power sets, explicit estimating equations, a finite BIC search, Lean-tracked algebra and R scripts that regenerate the reported evidence.

6.4 Limitations

Several limitations are left visible. The fish-nutrition data in Hubin et al. (2026) are a notational and methodological anchor, not a replicated application. The submitted implementation uses the second-order score; higher-order PMM-FP is theoretically supported but requires stronger moments and stabler matrix estimation. Lean checks the definitions, algebraic identities and conditional theorem structure, while the full M-estimator CLT and Schur-complement theory remain standard statistical inputs. Finally, small samples and very heavy tails can make residual cumulants noisy, so bootstrap uncertainty, trimming sensitivity and condition numbers should be reported before interpreting \hat{g}_2 as an efficiency forecast.

7 Conclusions

This paper gives a frequentist bridge from Kunchenko's polynomial maximization method to fractional-polynomial modelling. The bridge has three components: a two-track fractional residual basis, a PMM estimating score with the second-order variance ratio in (3.7), and a reproducible implementation that separates model selection from score-based coefficient estimation.

The practical message is simple. Use PMM-FP when the FP mean structure is scientifically

plausible and residuals are visibly non-Gaussian. The positive track is the stable default; the full track should be reported only with BD0, inverse-moment and condition-number diagnostics. When those diagnostics fail, the positive track still gives a transparent efficiency correction without treating negative powers as harmless.

All scripts needed to rebuild the reported tables, figures, R session information and Lean build evidence are listed in the supplement README .md. The GBSG dataset is public through mfp; the fish-nutrition data of [Hubin et al. \(2026\)](#) are not included and are not used for a replication claim.

References

- Akaike, H. (1973). Information theory and an extension of the maximum likelihood principle. In Petrov, B. N. and Csáki, F., editors, *Proceedings of the 2nd International Symposium on Information Theory*, pages 267–281, Budapest, 1973. Akadémiai Kiadó.
- Bickel, P. J., Klaassen, C. A. J., Ritov, Y., and Wellner, J. A. (1993). *Efficient and Adaptive Estimation for Semiparametric Models*. Johns Hopkins University Press, Baltimore. ISBN 978-0-801-84541-2.
- Boyd, S. and Vandenberghe, L. (2004). *Convex Optimization*. Cambridge University Press, Cambridge, UK.
- Crippa, A., Discacciati, A., Bottai, M., Spiegelman, D., and Orsini, N. (2019). One-stage dose-response meta-analysis for aggregated data. *Statistical Methods in Medical Research*, **28**(5), 1579–1596. doi:[10.1177/0962280218773122](https://doi.org/10.1177/0962280218773122).

- Godambe, V. P. (1960). An optimum property of regular maximum likelihood estimation. *Annals of Mathematical Statistics*, **31**(4), 1208–1211. doi:[10.1214/aoms/1177705693](https://doi.org/10.1214/aoms/1177705693).
- Hansen, L. P. (1982). Large sample properties of generalized method of moments estimators. *Econometrica*, **50**(4), 1029–1054. doi:[10.2307/1912775](https://doi.org/10.2307/1912775).
- Huber, P. J. (1981). *Robust Statistics*. John Wiley & Sons, New York. ISBN 978-0-471-41805-4. doi:[10.1002/0471725250](https://doi.org/10.1002/0471725250).
- Hubin, A., Krogdahl, Å., Løkka, G., and Kortner, T. M. (2026). Bayesian fractional polynomials for optimal dosage estimation with fish nutrition applications. URL <https://arxiv.org/abs/2605.06237>. arXiv preprint 2605.06237.
- Kunchenko, Y. P. (2002). *Polynomial Parameter Estimations of Close to Gaussian Random Variables*. Shaker Verlag, Aachen. ISBN 978-3-8322-0533-9.
- Ritz, C., Baty, F., Streibig, J. C., and Gerhard, D. (2015). Dose-response analysis using R. *PLOS ONE*, **10**(12), e0146021. doi:[10.1371/journal.pone.0146021](https://doi.org/10.1371/journal.pone.0146021).
- Royston, P. and Altman, D. G. (1994). Regression using fractional polynomials of continuous covariates: Parsimonious parametric modelling. *Journal of the Royal Statistical Society: Series C (Applied Statistics)*, **43**(3), 429–453. doi:[10.2307/2986270](https://doi.org/10.2307/2986270).
- Royston, P. and Sauerbrei, W. (2008). *Multivariable Model-building: A Pragmatic Approach to Regression Analysis Based on Fractional Polynomials for Modelling Continuous Variables*. John Wiley & Sons, Chichester. ISBN 978-0-470-02842-1. doi:[10.1002/9780470770771](https://doi.org/10.1002/9780470770771).
- Sabanés Bové, D. and Held, L. (2011). Bayesian fractional polynomials. *Statistics and Computing*, **21**(3), 309–324. doi:[10.1007/s11222-010-9170-7](https://doi.org/10.1007/s11222-010-9170-7).

- Sauerbrei, W., Royston, P., and Binder, H. (2007). Selection of important variables and determination of functional form for continuous predictors in multivariable model building. *Statistics in Medicine*, **26**(30), 5512–5528. doi:[10.1002/sim.3148](https://doi.org/10.1002/sim.3148).
- Schwarz, G. (1978). Estimating the dimension of a model. *The Annals of Statistics*, **6**(2), 461–464. doi:[10.1214/aos/1176344136](https://doi.org/10.1214/aos/1176344136).
- van der Vaart, A. W. (1998). *Asymptotic Statistics*. Cambridge Series in Statistical and Probabilistic Mathematics. Cambridge University Press, Cambridge. ISBN 978-0-521-78450-4. doi:[10.1017/CBO9780511802256](https://doi.org/10.1017/CBO9780511802256).
- Wang, L. and Leblanc, A. (2008). Second-order nonlinear least squares estimation. *Annals of the Institute of Statistical Mathematics*, **60**(4), 883–900. doi:[10.1007/s10463-007-0139-z](https://doi.org/10.1007/s10463-007-0139-z).
- Wedderburn, R. W. M. (1974). Quasi-likelihood functions, generalized linear models, and the Gauss–Newton method. *Biometrika*, **61**(3), 439–447. doi:[10.1093/biomet/61.3.439](https://doi.org/10.1093/biomet/61.3.439).
- Zabolotnii, S. (2025). Applying the polynomial maximization method to estimate ARIMA models with asymmetric non-Gaussian innovations. URL <https://arxiv.org/abs/2511.07059>.
- Zabolotnii, S., Tkachenko, O., Nowakowski, W., and Warsza, Z. L. (2025). Application of the polynomial maximization method for estimating nonlinear regression parameters with non-gaussian asymmetric errors. In *Automation 2024: Advances in Automation, Robotics and Measurement Techniques*, volume 1219 of *Lecture Notes in Networks and Systems*, pages 1–15. Springer, Cham. doi:[10.1007/978-3-031-78266-4_30](https://doi.org/10.1007/978-3-031-78266-4_30).

Zabolotnii, S. V. (2026). Parametrically adaptive transition polynomial: A signed-parity continuous- α extension of Kunchenko stochastic polynomials. URL <https://arxiv.org/abs/2605.14610>.

Zabolotnii, S. W., Warsza, Z. L., and Tkachenko, O. (2018). Polynomial estimation of linear regression parameters for the asymmetric PDF of errors. In *Automation 2018: Advances in Automation, Robotics and Measurement Techniques*, volume 743 of *Advances in Intelligent Systems and Computing*, pages 758–767. Springer, Cham. doi:[10.1007/978-3-319-77179-3_75](https://doi.org/10.1007/978-3-319-77179-3_75).

Zabolotnii, S. W., Warsza, Z. L., and Tkachenko, O. (2019). Estimation of linear regression parameters of symmetric non-Gaussian errors by polynomial maximization method. In *Automation 2019: Progress in Automation, Robotics and Measurement Techniques*, volume 920 of *Advances in Intelligent Systems and Computing*, pages 636–648. Springer, Cham. doi:[10.1007/978-3-030-13273-6_59](https://doi.org/10.1007/978-3-030-13273-6_59).